Iran J Sci Technol Trans Sci (2021) 45:1247–1261
https://doi.org/10.1007/s40995-021-01147-8

RESEARCH PAPER

Green Synthesis of Chitosan Bio-Nanocomposites and Investigation of their Antimicrobial and Antitumor Effects

H. S. El-Sheshtawy[1] · H. H. H. Hefni[1] · Wael A. Aboutaleb[1] · M. M. Elaasser[3] · M. F. Mady[2] · H. H. El-Shiekh[2]

Received: 27 August 2020 / Accepted: 14 May 2021 / Published online: 31 May 2021

Abstract

In the present study, silver, cadmium, iron and copper nanoparticles were biosynthesized by *Salmonella typhimurium, Staphylococcus aureus*, *Candida albicans and Fusarium avenaceum* strains. Analysis of the synthesized nanoparticles using the dynamic light scattering (DLS) revealed that the smallest nanoparticles were obtained by *Salmonella typhimurium*. The formation of the synthesized bio-AgNPs was confirmed by UV–Vis spectroscopy. The Ag, Cd, Fe and Cu nanoparticles produced by *Salmonella typhimurium* were separately immobilized on the chitosan (CS) framework by the impregnation method. The prepared CS-bio-nanocomposites were characterized by X-ray diffraction (XRD). The prepared compounds were investigated against three cancer cells (MCF-7, HeLa and HCT-1l6) for anticancer activity as well as against different microbial strains as antimicrobial activity. CS-bioAgNP composite clearly showed the greatest cytotoxicity against different cancer cell lines. Also, the CS-bioAgNP composite resulted in the highest inhibitory effect against different microbial growth strains using disk diffusion and kill time methods when compared with chitosan and other CS-bioNPs composites. Therefore, the present study provides evidence of novel antimicrobial and potent cytotoxicity characteristics of CS-bio-nanocomposite material that can be effectively utilized in the medical field.

Keywords Anticancer activity · Antimicrobial activity · Biosynthesis · Chitosan · Nanocomposite · Nanoparticles

1 Introduction

Metal nanoparticles with at least one dimension approximately 1–100 nm have received great attention in both metal nanoparticles with at least one dimension approximately 1–100 nm have received great attention in both technological and scientific areas due to their unique and unusual physicochemical properties (Vasileva et al. 2011). The importance of metal nanoparticles could be attributed to their catalytic activity, electronic characteristics, optical properties, antimicrobial, anticancer and magnetic activity (Khan et al. 2019). Furthermore, the bio-nanotechnology is arising and combines principles of biology with physical and chemical procedures to synthesize nano-sized particles with particular functions (Kathiresan et al. 2009). Over the past several years, the synthesis of various nanoparticles such as palladium, selenium, platinum, gold and silver using algae, fungi, bacteria and plant extracts has been reported (Torres et al. 2012), whereas the available chemical methods are often expensive and are comparatively complex, the synthesis of nanomaterials by biological agents is both economically and environmentally green as they are established on green chemistry basics and are simple, comparatively inexpensive and can be scaled up for larger-scale production. (Yasmin et al. 2020).

Despite the improvement in cancer treatment options, it remains a global burden that causes death of millions of people worldwide every year. One of the reasons causing the failure of cancer treatment is that many anticancer medications are unable to extend their target sites in

✉ H. S. El-Sheshtawy
hudaelsheshtawy@epri.sci.eg

[1] Egyptian Petroleum Research Institute (EPRI), El- Zohour Region, 1 Ahmed El-Zomor Street, Nasr City, Cairo 11727, Egypt

[2] Botany and Microbiology Department, Al-Azhar University, Nasr City, Cairo, Egypt

[3] Regional Center for Mycology and Biotechnology, Al-Azhar University, Nasr City, Cairo, Egypt

appropriate concentrations and efficiently exert the pharmacological impact without causing irreversible undesirable injury to healthy tissues and cells. Thus, modified antitumor drugs have advantages compared to traditional drugs including better delivery and lower doses (Pérez-Herrero et al. 2015).

Chitosan, a natural biopolymer, has attracted considerable attention due to its biological properties, such as antimicrobial, antitumor and immune-enhancing effects, besides being relatively cheap. The suggested mechanism for its antimicrobial action is bounding to the negatively charged bacterial cell wall, with subsequent destabilization of the cell envelope and altered permeability and finally by correlation with the repression of DNA replication (Gu et al. 2003; Dutta et al. 2011). The chitosan (CS) nanocomposite has attracted special consideration due to its biocompatibility and biodegradability. Additionally, the antimicrobial activity of chitosan nanocomposites against different groups of microorganisms, such as Gram-negative and Gram-positive bacteria (such as *Escherichia coli, Proteus mirabilis, Pseudomonas aeruginosa and Staphylococcus aureus*), has received considerable attention due to their impact on food and healthcare industries (Wei et al. 2009; Thomas et al. 2009).

In the present study, the extracellular synthesis of metal (Ag, Cd, Fe and Cu) nanoparticles by four microbial strains (*Salmonella typhimurium, Staphylococcus aureus, Candida albicans and Fusarium avenaceum*) was investigated. The microbial strain producing the lowest size of metal nanoparticles was then selected. The biologically synthesized metal nanoparticles were immobilized on chitosan polymer for the enhancement of its antimicrobial and anticancer properties.

2 Materials and Methods

2.1 Materials

2.1.1 Chemicals

All the chemicals used in this study were of analytical grade. Sodium hydroxide (NaOH), silver nitrate ($AgNO_3$), cadmium nitrate ($Cd(NO_3)_2$), ferric chloride, copper sulfate ($CuSO_4.5H_2O$), barium chloride, glacial acetic acid (99.5%), Tween 80 MTT [3-(4,5-Dimethylthiazole-2-yl)-2, 5-diphenyl tetrazolium], Triton X-100 and sodium thiosulfate were purchased from Sigma-Aldrich (Steinheim, Germany). The Muller-Hinton-Broth and potato-dextrose agar media were purchased from OXOID LTD (Hampshire, England). Chitosan was purchased from Egyptian Petroleum Research Institute (EPRI) (Motawie et al. 2014).

2.1.2 Bacterial and Fungal Strains

Salmonella typhimurium (*S. typhimurium* ATCC 14,028), *Staphylococcus aureus* (*St. aureus* ATCC 25,923) bacterial strains were obtained from TCS Biosciences Ltd, England. Moreover, *Candida albicans* (*C. albicans* ATCC 10,231) and *Fusarium avenaceum* (*F. avenaceum* DMS 62,161) strains were obtained from the Regional Center for Mycology& Biotechnology, Al-Azhar University, Nasr City, Cairo, Egypt.

2.1.3 Cell Lines

Human carcinoma cell lines; MCF-7 cells (human breast carcinoma), HeLa cells (human cervical carcinoma) and HCT-116 cells (human colon carcinoma) were obtained from the American Type Culture Collection (ATCC, Rockville, MD). The cells were grown on RPMI-1640 medium supplemented with 10% inactivated fetal calf serum and 50 µg/ml gentamycin (Lonza, Belgium). The cells were maintained at 37 °C in a humidified atmosphere with 5% CO_2 and were sub-cultured two to three times a week during the period of experiment.

2.2 Methods

2.2.1 Maintenance Media of Tested Microorganisms

The bacterial strains *S. typhimurium* and *St. aureus* were maintained at 4 °C on nutrient agar slants. The fungal strains *C. albicans* and *F. avenaceum* were maintained at 4 °C on potato-dextrose agar slants.

2.2.2 Growth Media for the Production of Nanoparticles

Microbial test strains were inoculated in Muller-Hinton-Broth (MH) (g/L): Beef dehydrated infusion, 300.0; Casein hydrolysate, 17.5; starch, 1.5 and adjusted pH 7.3 ± 0.1. The cultivation of tested microbial strains was carried out by 1 ml fresh microbial culture suspension corresponding to 10^6 CFU/mL inoculated in autoclaved Muller-Hinton-Broth and incubated at 37 °C for 18–24 h for bacterial strains while incubated at 28 °C for 5–7 days in case of fungal stains. After the incubation period, the mycelium of fungus *F. avenaceum* was separated by vacuum filtration on Whatman (42ASHLESS) filter paper. On the other hand, yeast and bacterial culture supernatants were collected by centrifugation at 5000 rpm for 30 min at room temperature and then filtrated by membrane-filtration using vacuum and the cell-free supernatants were collected for further studies. The autoclaved Muller-Hinton-Broth media without inoculation were used to check the sterility of media.

2.2.3 Extracellular Synthesis of Nanoparticles Using Microbial Strains

The extracellular synthesis of different nanoparticles [Cu-NPs, Cd-NPs, Ag-NPs and Fe-NPs] was performed by adding 1 mM $CuSO_4.5H_2O$, $Cd(NO_3)_2$, $AgNO_3$ and $FeCl_3$ as nanoparticle precursors, respectively, to the harvested culture supernatants with a volume ratio of 10:100. In the synthesis of Fe-NPs, 1 mM $FeCl_3$ was used as mentioned before and then 5 M NaOH was added slowly with magnetic stirring till obtaining a brown precipitate.

$$1\text{mM } FeCl_3 + \ 5\text{M NaOH} \rightarrow Fe\ (OH)_3 + 3\text{NaCl} \downarrow$$

On the other hand, for the synthesis of Cd-NPs, 1 mM $Cd(NO_3)_2$ was used and then 1 mM of $Na_2S_2O_3$ was added slowly with magnetic stirring at 45 °C. All mixtures were incubated at ambient temperature and maintained in the dark for 24 h to avoid light effects. At the end of incubation, the mixture was centrifuged at 5000 rpm for 30 min to precipitate the harvest metals-NPs and then washed with deionized water and dried in the oven at 65 °C for 24 h. A control experiment was conducted using un-inoculated media to check for the role of bacteria in the synthesis of nanoparticles (Sunkar and Nachiyar 2012).

2.2.4 Preparation of Chitosan Bio-nanoparticles (CS-Bio-nanocomposite)

Chitosan solution (1%) was prepared by dissolving 0.5 g of chitosan [with molecular weight 110 Kda and degree of deacetylation $\geq$ 80%] in 50 mL of acetic acid aqueous solution (2%). The mixture was stirred for 20 min at room temperature to obtain a homogeneous viscous solution, filtered through polyester cloth to remove residues of insoluble particles. 0.5 g of dried Cu, Ag, Fe and Cd-NPs was added separately to the mixture of chitosan solution and stirred at 1000 rpm and 60 °C for 1 day, the pH of solutions was adjusted to neutralization by 0.5 M NaOH solution. Each solution was centrifuged for 20 min at 5000 rpm to separate the solid products which were washed several times with distilled water and then dried in the oven at 40 °C for 24 h.

2.2.5 Characterization of the Prepared CS-Bio-nanocomposite

The crystal structure of the prepared pure metal bio-nanoparticles and chitosan-metal bio-nanocomposites was analyzed using the X-ray diffraction technique. The XRD experiments for the prepared samples were carried out using the X'pert Pro PANalytical apparatus. The apparatus is equipped with Cu Kα radiation (λ = 0.15418 nm). The patterns were recorded in 2θ rang of 10–80° with a rate of 0.05 s^{-1}. The crystal size was calculated from Scherer's equation as ($d = 0.9\ \lambda\ /\ \beta\ \cos\theta$); where the λ is X-ray wavelength, β is the half-full maximum intensity in radians and θ is Bragg's angle in radian.

The prepared sample's particle sizes were determined by the dynamic light scattering analytical method. The particle sizes were measured by using a Zetasizer Nano instrument supplied by Malvern Instruments Ltd. For these popups, 3 mg sample was dissolved in 10 mL water and subjected to ultra-sonication for 5 min for stable suspension formation. The sample was then loaded into the cell area on the top of the instrument. The cells were then subjected to a laser beam to measure the luminescence. The particle size distribution curve was then taken by the apparatus software. The measurement was repeated five times for each sample to ensure the reproducibility.

To conform the formation of Ag-Nps was carried out using the ultraviolet–visible (UV–Vis) spectroscopy with Shimadzu UV-2550 double beam system, Japan (Badr et al. 2021).

2.2.6 Cytotoxicity of Chitosan (CS) and the Prepared (CS-bio-nanocomposites) Against Different Tumor Cells

For cytotoxicity experiments, each of the carcinoma cell lines (MCF-7, HeLa and HCT-116 cells) was seeded in 96-well plate at a density of 10,000 cells/cm^2. Six different concentrations of chitosan (CS) and CS-bio-nanocomposites were prepared by dilution with the RPMI 1640 growth media. After reaching 90% confluence, the cells were washed with PBS buffer and then 100 µL of the investigated concentration of CS and CS-bio-nanocomposites was added and incubated along with tissue cultured wells without any nanoparticle as a negative control and cells treated with Triton X-100 as a positive control for a period of 24 h. Cytotoxicity of the synthesized preparation was evaluated using MTT assay. Briefly, 5 mg of MTT [3-(4, 5-Dimethylthiazole-2-yl)-2, 5-diphenyl tetrazolium] was dissolved in 1 mL of PBS and filter sterilized. 10 µL of the prepared MTT solution was further diluted to 100 µL with 90 µL of serum-free phenol red-free minimum essential medium (MEM). The cells were incubated with the diluted MTT solution for 4 h. Formazan crystals produced by viable cells were dissolved by replacing the MTT-containing medium with 100 µL of the solubilization solution (10% Triton X-100, 0.1 N HCl and isopropanol). After 1 h incubation at room temperature, the optical density was determined at a wavelength of 570 nm by the microplate reader (SunRise, TECAN, Inc, USA) and the percentage of viability was calculated as [(ODt/ODc)] × 100% where ODt is the mean optical density of wells treated with the tested sample and ODc is the mean optical density of

untreated cells. Triplicate samples were examined for each experiment.

2.2.7 Antimicrobial Activity of Chitosan (CS) and the Prepared CS-bio-nanocomposites

The antimicrobial activities of CS and CS-bio-nanocomposite were conducted against *Escherichia coli, Salmonella typhimurium, Pseudomonas aeruginosa, Staphylococcus aureus and Candida albicans.* Prolonged period conservation of the microbial strains was at -20 °C using glycerol and short period conservation was on nutrient agar plates at 4 °C. The solutions of CS and CS-bio-nanocomposite compounds were prepared as follows: 1 gm of each compound was dispersed in 100 mL of 1% (v/v) acetic acid solution with stirring overnight until completely soluble. The pH was adjusted at 5.8 using 5 M NaOH (the pH most adequate to solubilize chitosan and without any antibacterial effect). Then, the solutions were autoclaved at 120 °C for 15 min.

2.2.7.1 Disk Diffusion Method Based on European Committee for Antimicrobial Susceptibility Testing (EUCAST) of the European Society of Clinical Microbiology and Infectious Diseases (ESCMID), the disk diffusion method was performed using filter paper disks which were saturated with the tested concentrations of CS and CS-bio-nanocomposite compounds and then applied to the surface of MH agar medium that has been seeded with the examined microorganisms. The microorganisms were inoculated onto agar plates using a sterile cotton swab, streaked in three directions over the entire agar surface. Using a sterile forceps, antimicrobial disks (saturated with CS and CS-bio-nanocomposites) were applied onto the agar plate's surfaces and placed at an equal distance apart from each other. The plates were inverted and incubated within 15 min after disks were applied at 35 °C. After the incubation period till 18 h, the clear zone's diameters were measured for recording the inhibition activities of CS and CS-bio-nanocomposites against tested microorganisms compared to blank disks (Mohsen et al. 2020).

2.2.7.2 Kill Time Method In this experiment, bactericidal and fungicidal activities were determined by the investigated concentrations of CS and CS-bio-nanocomposites. Cultures of tested microbial strains were exposed to CS and CS-bio-nanocomposites for a known time and then tested strains were re-cultured on nutrient agar media. The incubation is done under suitable conditions for varied time intervals (0, 30, 60, 90 and 120 min). Then, the percentage of dead cells is calculated relatively to the growth control by determining the number of living cells (CFU/mL) of each tube using the agar plate count method (Konaté et al. 2012).

2.2.8 Statistical Analysis

Differences among the different metal nanoparticles' activities, as measured by the inhibition zones, were analyzed using two-way ANOVA (Microorganisms and materials), followed by Tukey's comparisons in order to determine the best effective material that achieve high inhibition zones (Bastos et al. 2008; Al-Ostoot et al. 2018). The standard deviation was calculated and plotted on the graph where two replicates have been used throughout the experiment.

3 Results and Discussion

Extracellular biosynthesis of Ag, Cd, Fe and Cu nanoparticles was investigated using different microorganisms; i.e., *Salmonella typhimurium* (as a Gram-negative bacterium of the family *Enterobacteriaceae), Staphylococcus aureus* (as a Gram-positive bacterium and member of the *Firmicutes), Candida albicans* yeast (as unicellular fungi) and *Fusarium avenaceum* (representing filamentous fungi). The produced bio-nanoparticles were immobilized on chitosan and evaluated for their cytotoxicity and antimicrobial applications.

Biosynthesis refers to the phenomena which take place by biological routes or through enzymatic reactions. These eco-friendly processes, referred to as green technology, can be used to achieve better metal nanoparticles using microbial cells (Mandal et al. 2006).

The extracellular biological synthesis of metal nanoparticles by the investigated microbial strains resulted in NPs formation of different sizes, which might be attributed to the existence of different types of enzymes excreted from these organisms through the biosynthesis processes as previously reported by Ovais et al. (2018). The dynamic light scattering (DLS) data were collected, and related results are represented in Fig. 1. The DLS results show that smallest particle size among the prepared metal nanoparticles (Ag, Cd, Fe and Cu) was achieved by *Salmonella typhimurium* (24.11, 32.44, 107.3, 38.77 mm, respectively). The results have shown that silver nanoparticles possessed the smallest size nanoparticles by *S. typhimurium,* which is characterized not only by its high ability to produce nanometals but also by producing the smallest particle size when compared with the other investigated microbial strains synthesizing nanoparticles. Using dynamic light scattering analysis, Ghorbani (2013) found that the size of the produced silver nanoparticle by *S. typhimurium* was 87 ± 30 nm. Therefore, *Salmonella typhimurium* was selected for further analyses.

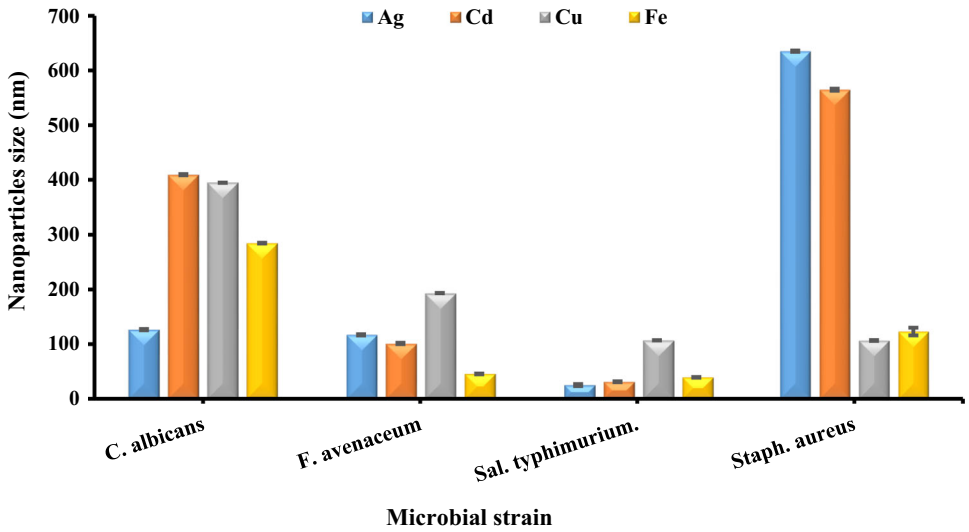

Fig. 1 Different metal nanoparticles size prepared by different microbial strains

3.1 Formation and Characterization of bio-AgNPs

The results presented in Fig. 2 show the color change of silver metal ion after the formation of nanoparticles. The color of Ag ion changed from whitish to yellowish-brown indicating the reduction effect of bacterial enzymes. The observed color changes are consistent with previous studies by others (Ghorbani 2013; SuÃrez-Cerda et al. 2017).

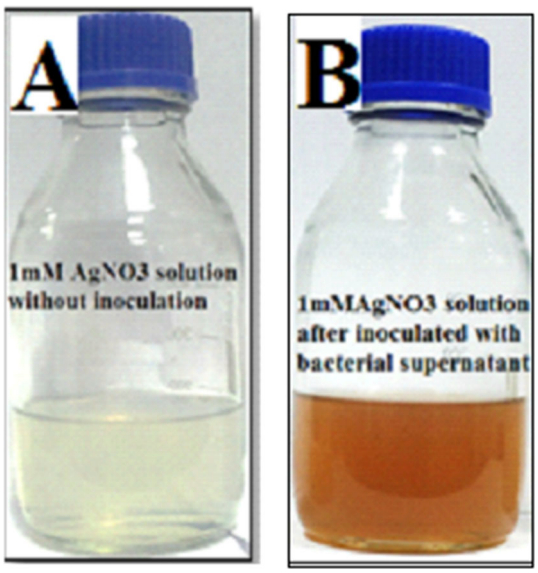

Fig. 2 Silver nitrate (1 mM) solution before (A) and after (B) incubation with the supernatant of *Salmonella typhimurium*. Photograph (A) shows the color of silver metal ion solution as blank, photograph (B) is the color of silver metal ion after incubation in inoculated media. The color of Ag ion changed from whitish to yellowish-brown, indicating the reduction effect of bacterial enzymes

3.1.1 UV–Vis spectroscopy of the Biosynthesized AgNPs

Depending on the surface plasmon resonance (SPR) of free surface electrons, the UV spectra from the UV–Vis spectrophotometer showed the structure of the bio-AgNPs. In Fig. 3, the spectra of bio-AgNPs revealed a distinct absorption band at 475 nm. In the SPR band, the peak indicated the size and shape of bio-AgNPs (Mlalila et al. 2017; Kumar et al. 2017).

3.2 Characterization of Bio-NPs and CS-Bio-nanocomposites

The immobilization of bio-nanoparticles on chitosan in order to increase their antibacterial and cytotoxicity capabilities. The reason for choosing chitosan is that chemical alterations of chitosan are mostly preferred to progress the polymer process capability as well as to modulate some of its properties such as cytotoxicity and antimicrobial activity. Moreover, chitosan can interact with metal and metal nanoparticles through coordination bonds with its functional groups such as NH_2 and OH (Hussein et al. 2012). These interactions with nanometal zero Valente could be through capping (Usman et al. 2012), as seen in Fig. 4.

3.2.1 X-ray Diffraction (XRD)

The powder XRD patterns for the prepared nanocomposites were recorded as shown in Fig. 5. Fig. 5a shows broad peaks at 2θ of 11.7°, 20.2°, which assigned for chitosan as documented previously in the literature (Kong et al. 2005; Wang et al. 2004). The peaks broadening and higher intensity were attributed to the partial crystallinity of chitosan nature. Moreover, no additional peaks other than

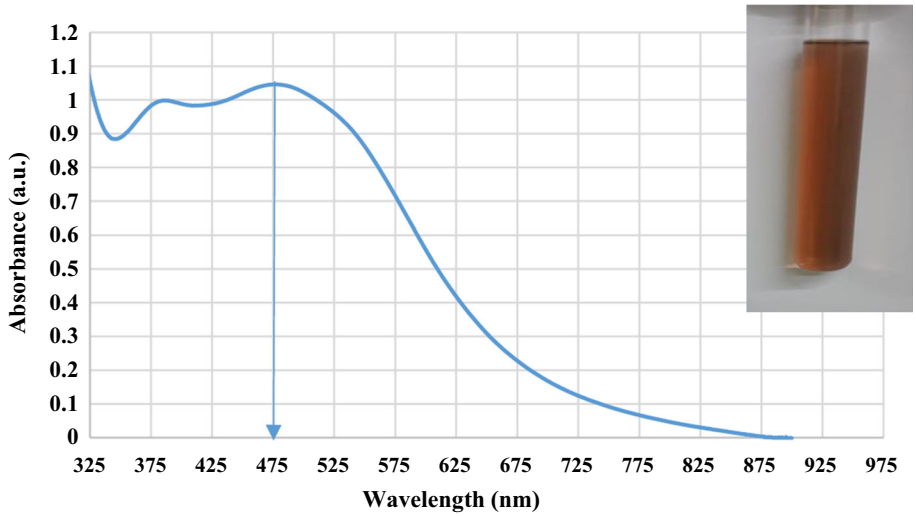

Fig. 3 UV–Vis spectra of the biosynthesized silver nanoparticles (AgNPs)

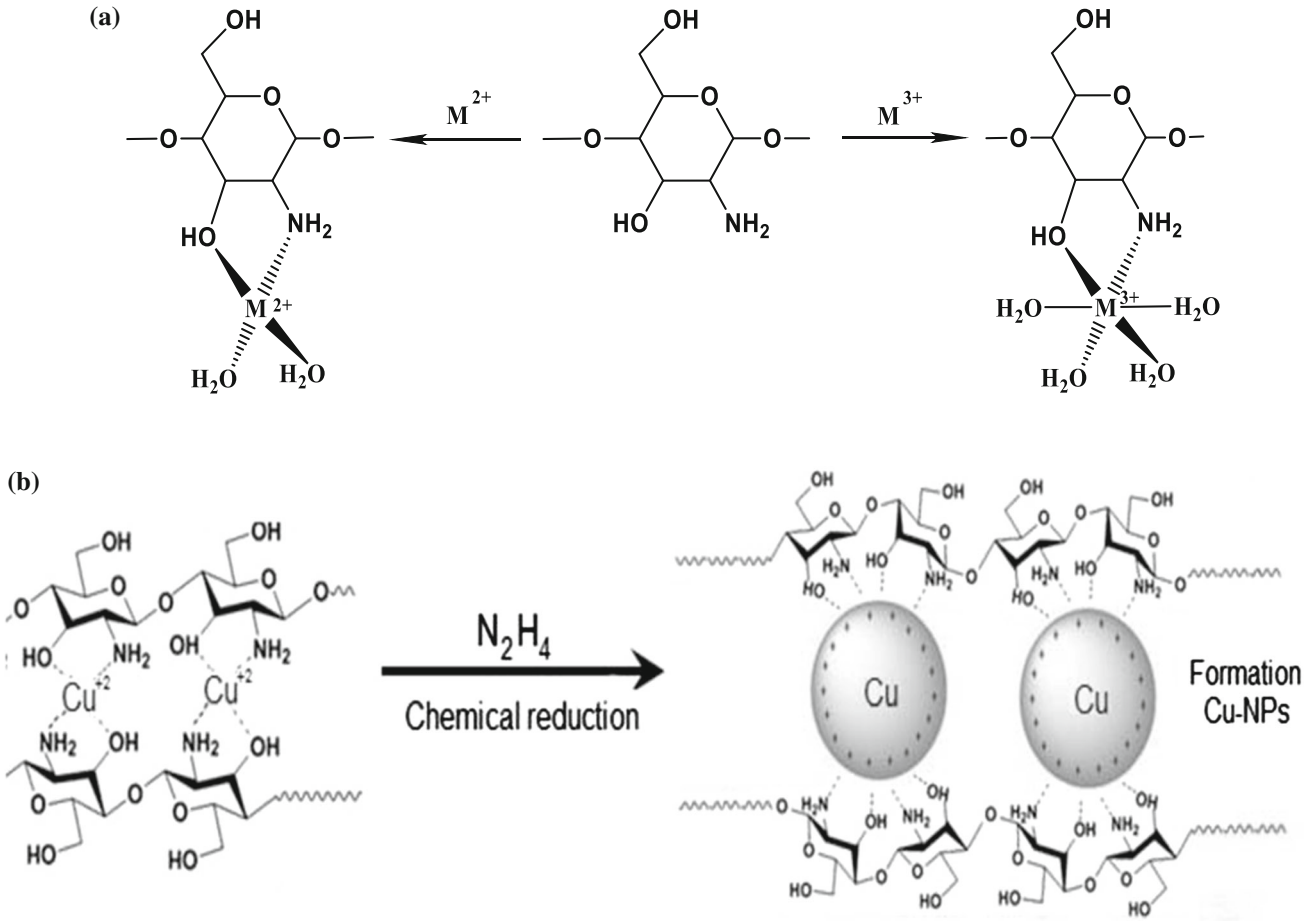

Fig. 4 The structures of interaction between chitosan and metals **a** and with zero-valent nanometals **b**

chitosan were recorded indicating the polymer's high purity. On the other hand, Fig. 5b represents the XRD patterns for the prepared pure Cu nanoparticles. The diffractogram showed definite peaks at 43.3° and other tiny peaks at 50.5° and 74.08° which characterize the face-centered cubic metallic Cu particles. The mentioned peaks expressed the 111, 110 and 200 line indexed copper (Mott et al. 2007). Moreover, some of the other peaks at around 28°, 31.5°, 37.5° corresponding to the $Cu(OH)_2$ and CuO, respectively, were detected. Additionally, well-recognized

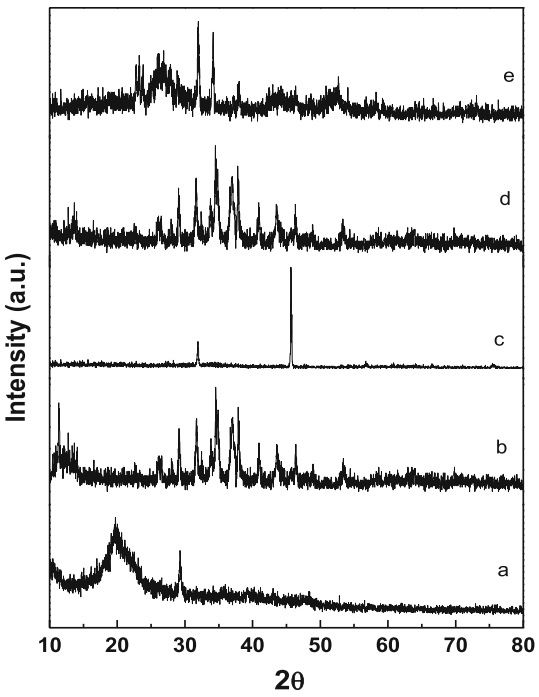

Fig. 5 The X-ray diffraction analyses of the as-prepared **a** chitosan and loaded chitosan with **b** Cu, **c** Fe, **d** Ag and **e** Cd nanoparticles produced by *Salmonella typhimurium*

peaks at 36.4° and 42.5° were observed and may attribute to the Cu_2O phase (Li et al. 2017; Liu et al. 2016). Those other peaks showed the incomplete Cu precursor conversion to Cu particles and some formed metal oxidation. This observation reflects that the synthesis process should be carried out for a longer time for full conversion. Also, the formation of CuO may be attributed to the fast oxidation ability of the formed Cu particles. The X-ray patterns of the prepared Fe nanoparticles are recorded and shown in Fig. 5c. The diffractogram showed a high intense and very sharp peak at 45.6° which is characteristic of the zero-valent iron nanoparticles (Yuvakkumar et al. 2011). The characteristic peak sharpness indicated that they formed iron high crystallinity. Additionally, a tiny peak at around 32° may be attributed to the tiny formation of Fe_3O_4 particles. Meanwhile, the intensities of the peaks indicated that the zero-valent iron nanoparticle predominantly existed. The XRD patterns of the prepared Ag nanoparticles are recorded and shown in Fig. 5d. The data showed considerable peaks at 37.9° and 44.2°, which correspond to the (111) and (002) plans of the cubic structure pure silver nanoparticles (Jbeli et al. 2018; Mukherjee et al. 2017). Also, a small peak at 64.6° that indexed the (220) plan was recorded. Additionally, other diffraction peaks around 2θ of 31.5° and 34.5°, which could be attributed to the $AgCO_3$, were also found (Raffi et al. 2008). The carbonate species may be formed due to the rich CO_2 environment resulted from the bacterial strain metabolism. So, it is better to preserve the samples under vacuum. The XRD diffractogram of the as-prepared CdS is shown in Fig. 5e. The figure showed wide broad peaks at 26.8°, 43.9° 48.1° and around 52° which match the (100), (111), (103), (220) and (311) faces of hexagonal CdS crystal.

The Cu-loaded chitosan spectrum showed (Fig. 6b) the peaks of Cu nanoparticles and a small peak at 2θ of 20.2° corresponding to the chitosan which prove the Cu loading to the chitosan framework. The peaks corresponding to the CuO and Cu_2O were also observed in the Cu-loaded chitosan. On the other hand, the X-ray diffraction profile of the chitosan-loaded iron oxide nanoparticles (Fig. 6c) showed very tiny peak at 20.2° corresponding to the chitosan which reflects the good distribution of the iron nanoparticles on the chitosan surface. Additionally, the main characteristic peak of zero-valent iron nanoparticles at 45.6° was too much weakened when the particles were loaded to chitosan. This observation can be attributed to the good homogony and uniform distribution of particles in the chitosan framework. More additional peaks were observed in the iron-loaded chitosan sample which attributed to the formation of hematite and magnetite due to the loading process. The powder X-ray diffraction of the Ag-loaded chitosan (Fig. 6d) showed peaks at 37.9° and 44.2° attributed to the Ag particles and peaks at 11.7° and 20.2° corresponding to the chitosan.

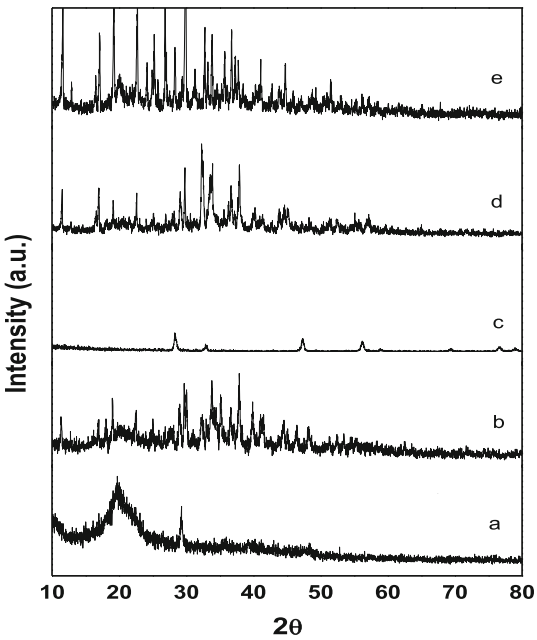

Fig. 6 The X-ray diffraction patterns of the **a** chitosan, **b** Cu, **c** Fe, **d** Ag and **e** Cd bio-nanoparticles by *Salmonella typhimurium*

3.3 Applications of Chitosan Bio-Nanocomposite (CS-bioNPs)

3.3.1 Cytotoxicity of CS-BioNPS against Different Tumor Cell Lines

The cytotoxicity of chitosan is attributed to the nature of its structure. Chitosan possesses high cationic charge densities due to its positively charged amino groups that can result in electrostatic ionic interaction with the negatively charged groups of tumor cells. Hence, chitosan could be adsorbed onto the negatively charged tumor cell membrane by electron interaction, subsequently exhibiting anti-tumoral effects via damaging membrane, organelles and finally lead to cell death (Li-Feng et al. 2005).

When chitosan is incorporated with metal nanoparticles (MNPs), it is expected to increase the cytotoxicity effect for incorporated materials, due to the nature of both chitosan and metal nanoparticles. The cytotoxicity of MNPs is due to their chemical structure (purity, crystallinity, electronic properties, etc.), small size (surface area and size division), surface framework (surface reactivity, surface groups, inorganic or organic coatings, etc.), shape, solubility and accumulation (Schrand et al. 2010).

In the present work, the cytotoxicity of CS-bioNPs composites produced by *Salmonella typhimurium* was evaluated against three human tumor cell lines; breast carcinoma cells (MCF-7), cervical carcinoma cells (HELA) and Colon carcinoma cells (HCT-116), showing dose-dependent cell killing as can be seen in Fig. 7. It is clear from these figures that the cytotoxicity of CS-bioNPs composites against tumor cells decreased in the order CS-AgNPs > CS-FeNPs > CS-CuNPS > CS-CdNPs.

The greater cytotoxicity effect of CS-AgNPs composite against all tested tumor cell lines is due to the nature of the silver atom, which has great ability to produce reactive oxygen species (ROS) and oxidative stress (Schrand et al. 2010) and has a great potential in cancer management due to possessing an active physicochemical interaction with the functional groups of intracellular proteins, as well as with the nitrogen bases and phosphate groups in DNA (Satyavani et al. 2011). AgNPs are selectively involved in the disruption of the mitochondrial respiratory chain leading to the production of ROS and interruption of adenosine triphosphate (ATP) synthesis, which in turn cause DNA damage (Asha-Rani et al. 2009; Sriram et al. 2010).

On the other hand, the cytotoxic effects of the CS-FeNPs are due to their structure that contains nano-zero-valent iron (nZVI Fe^0) as mentioned in XRD discussion. The mechanism for cellular damage is considered to be regarded as nZVI oxidation reactions, where redox cycling and the generation of ROS from reduced Fe within a cell can cause lipid peroxidation and DNA damage (Xia et al. 2006).

Additionally, Cu nanoparticles can also diffuse into the cell directly through cell membrane pores, or they can enter through ion channels and transporter proteins on the plasma membrane. Different types of nanoparticles may enter into cells by endocytosis; a process where the membrane wraps around and vesicles transport nanoparticles into cells. Nanoparticles that enter the cell may associate directly with oxidative organelles like mitochondria. Later, redox-active proteins promote the formation of reactive oxygen species (ROS) in cells and nanoparticle-produced ions (Cu^{2+}) may stimulate ROS through a variety of chemical reactions. ROS has the ability to cause DNA strand breaks and change gene expression. Cu^{2+} ions can also form chelates with biomolecules or dislodge metal ions from particular metalloproteins, resulting in functional protein inactivation. Cu^{2+} released by copper oxide nanoparticles enhances local concentrations and disrupts cellular metal cation homeostasis, causing cell toxicity (Avinash et al. 2014). Despite the CuNPs had the strong cytotoxicity effect as mentioned above, CS-CuNPs showed the smallest cytotoxicity impact than both CS-AgNPs and CS-FeNPs. It is due to the biggest size of nanoparticles of CS-CuNPs > 100 nm than other CS-MNPs. It may be also attributed to the conversion of the most biosynthesis Cu^0, which is responsible for the formation of reactive oxygen species (ROS) to Cu^{2+}, through the addition of chitosan, as illustrated in XRD section.

CdNPs here also induced significant ROS generation with exposure time (L'Azou et al. 2014). Acute Cd exposure can increase oxidative stress by producing superoxide anions and nitric oxide. Cd has been shown to induce lipid peroxidation and cause excretion of lipid metabolite in urine (Pujalté et al. 2011). Also, CS-CdSNPs have shown the lowest cytotoxic effects among the other CS-MNPs compounds that may be attributed to smaller nano-size of its structure leading to instability (Jin and Zhao 2009).

3.3.2 Antimicrobial Activities Measurements of CS and Chitosan Bio-Nanocomposite (CS-bioNPs)

The antimicrobial action of chitosan has been postulated. The chitosan could chelate with trace elements or essential nutrients so as to inhibit the growth of bacteria (Barry et al. 1999). Chitosan could interact with anionic groups on the cell surface and form polyelectrolyte complexes with bacterial surface compounds, thereby forming an impermeable layer around the cell, which prevents the transport of essential solutes into the cell (Roller et al. 1999). Chitosan nanoparticles exhibit higher antibacterial activity than chitosan on account of the special character of the nanoparticles (Muzzarelli et al. 1990). The negatively

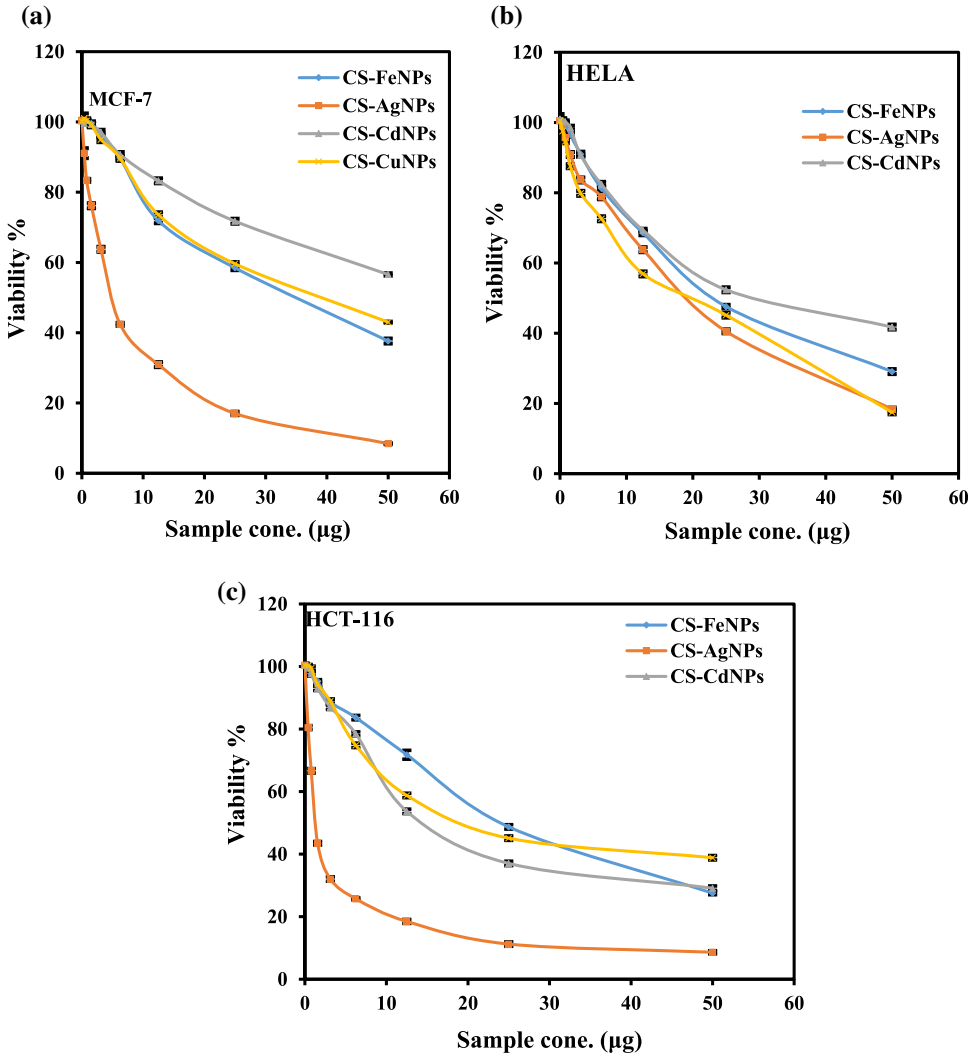

Fig. 7 Effect of CS-bioNPs concentrations on cell vaibility of **a** MCF-7 **b** HELA **c** HCT-116 tumor cells; showing dose response curves indicating concentration-dependent inhibition of tumor cell viability by the tested nanoparticles preparations

charged surface of the bacterial cell is the target site of the polycation. Therefore, the polycationic chitosan nanoparticles with higher surface charge density interact with the bacteria to a greater degree than chitosan itself. Chitosan nanoparticles provide higher affinity with bacteria cells for a quantum-size effect. Because of the larger surface area of the chitosan nanoparticles, nanoparticles could be tightly adsorbed onto the surface of the bacteria cells so as to disrupt the membrane, which would lead to the leakage of intracellular components, thus killing the bacteria cells (Bong-Kyu et al. 2001).

The antimicrobial activities of CS and CS-bioNPs composites were examined and explained by two different methods as follow:

3.3.2.1 Disk Diffusion Method In the disk diffusion method of susceptibility testing (known as the Kirby-Bauer method), filter paper disks impregnated with a specific amount of antimicrobial agents are applied to the surface of MH agar medium. The rate of diffusion of the antimicrobial during the agar is based on the diffusion and solubility properties of the antimicrobial in MH agar and the molecular weight of the antimicrobial component (Chung et al. 2004). The larger molecular weight of antimicrobial compounds will diffuse slower than lower molecular weight compounds. These factors result in each antimicrobial having zone size indicating susceptibility to that antimicrobial compound.

The formation of inhibition zones evaluated by the disk diffusion assay is shown in Table 1 and Fig. 8. The antimicrobial activity of chitosan (CS), bioNPs and CS-bioNPs composites against all of the examined microbial strains: *S. typhimurium*, *P. aeruginosa*, *E. coli*, *St. aureus and C. albicans* showed variable sensitivities, as it appears all microbial strains are susceptible to chitosan bio-nanocomposite with the gradient in inhibition zones resulted in the type of organism. CS-bio-nanocomposites disk showed a very clear inhibitory effect against Gram-

Table 1 Antimicrobial activity of chitosan and chitosan bioNPs composites against different microbial strains under study

Microorganisms	CS	CS-AgNPs	CS-CuNPs	CS-FeNPs	CS-CdNPs
	Inhibition zone (mm) (Mean ± SD)				
E. coli	13 ± 0.11	23 ± 0.40	19 ± 0.31	14 ± 0.23	14 ± 0.17
Sal. typhimurium	10 ± 0.13	21 ± 0.36	17 ± 0.27	9 ± 0.11	10 ± 0.15
P. aeruginosa	10 ± 0.15	22 ± 0.25	17 ± 0.30	12 ± 0.20	12 ± 0.20
St. aureus	16 ± 0.22	25 ± 0.24	17 ± 0.22	17 ± 0.28	17 ± 0.30
C. albicans	7 ± 0.14	27 ± 0.37	21 ± 0.35	9 ± 0.15	9 ± 0.10

SD is standard deviation

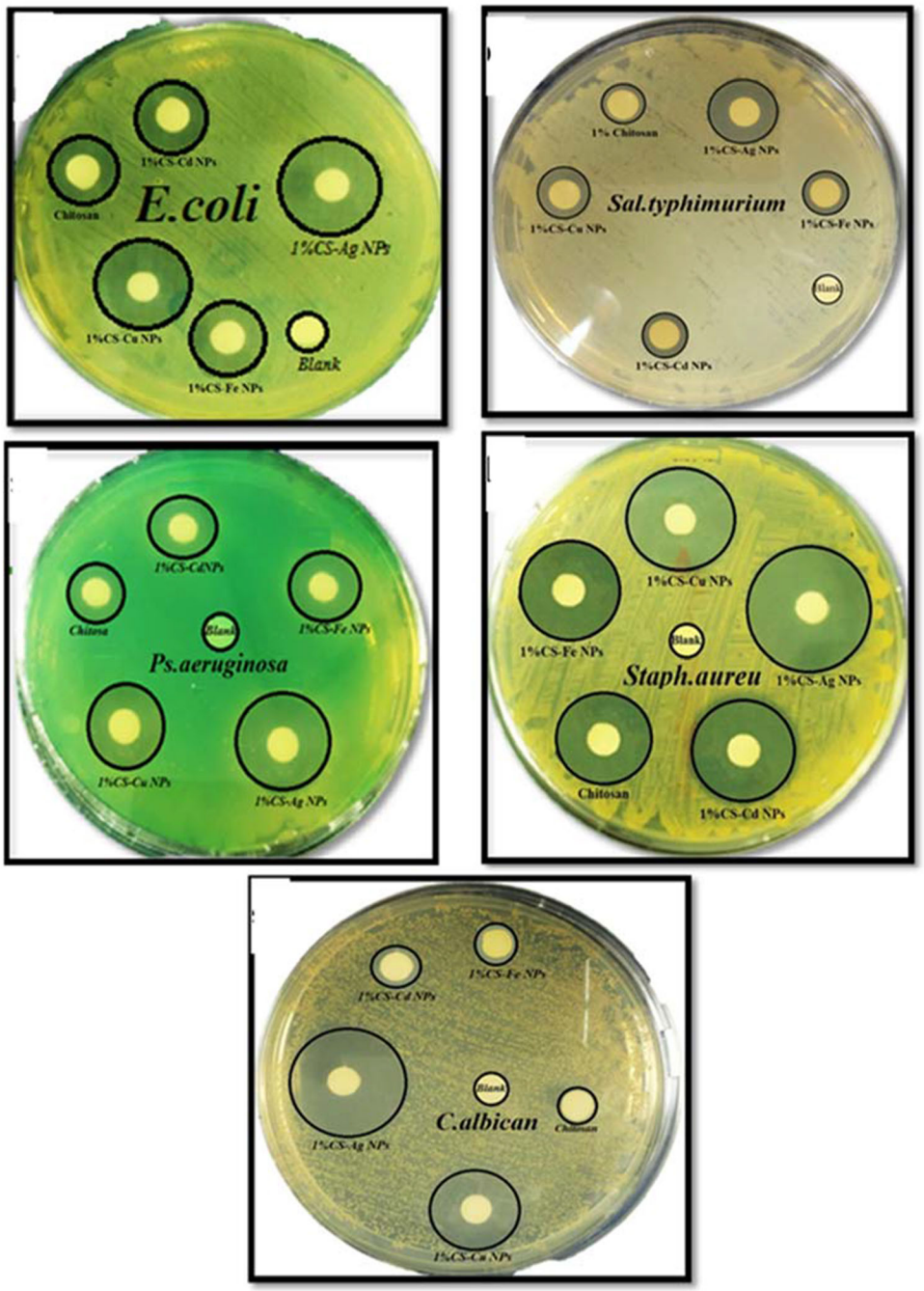

Fig. 8 Antimicrobial activities of CS and CS-bio-nanocomposites observed as inhibition clear zones against tested microbial strains compared to the corresponding bank

negative and Gram-positive bacterial strains and yeast strain than the chitosan film alone (Shahverdi et al. 2007; Kim et al. 2009). On the other hand, the CS-bioAgNP composite exerted the highest growth inhibitory effect against all microbial strains. However, Kaur et al. (2019) reported that the AgNPs are the most common metal NPs that explained the ability to inhibit the bacterial growth and interestingly displaying minimal toxic effect to human cells. The positive charge of Ag^{+} interacts with the negative charge on the cell wall of bacteria, causing changes in cell wall shape as well as an increase in cell permeability or leakage, which leads to cell death, according to Dakal et al. (2016). AgNPs have a higher affinity for phosphorous and sulfur-containing biomolecules found in extracellular (membrane protein) and intracellular (DNA bases, protein) components. These biomolecules have an effect on cell division and cell survival.

3.3.3 Statistical analysis

The confidence intervals in Table 1 at 95%, both the microorganisms and metals nanoparticles, were stated as significant factors which affect the inhibition zones for the organisms, where the P value was recorded as 0.035, $0.000 < 0.05$ for microorganisms and metals nanoparticles, respectively. Table 2 shows the coded coefficient for the factor levels and their P value results. Additionally, Tukey's comparisons showed that CS-AgNPs were the highly significant nanometals that achieve high inhibition zone followed by CS-CuNPs metal nanometal and the last three nanometals nearly have the same effects (see Table 2).

3.3.3.1 Kill Time Method The time-kill test is the most suitable method for determination the bactericidal or fungicidal effect. It is a strong tool for obtaining information about the dynamic interaction between the antimicrobial agent and the microbial strain. The time-kill test reveals a time-dependent or a concentration-dependent antimicrobial effect (Balouiri et al. 2016). In this study, bactericidal activity was determined by the known concentration of chitosan (CS) and CS-bioNPs composites were tested against a standard inoculum of microorganisms. The incubation was done under suitable conditions for varied time intervals (0, 30, 60, 90 and 120 min). After that, the number of living cells (CFU/mL) of each tube was calculated by using agar plate counts as seen in Fig. 9. The data illustrate that the exhibition of the studied microbial strains to CS and CS-bioNPs composites at different time intervals, the lowest microbial growth was determined after 120 min. This could be explained by the fact that the ability of CS and CS-bioNPs composites to penetrate the cell wall more easily and thus appeared with an enhanced antimicrobial activity (Sunkar et al. 2012). The percentage reduction of microbial growth caused after exposure to CS and CS-bioNPs composites at 120 min is shown in Table 3. The antimicrobial effect of CS and CS-bioNPs composites on Gram-negative bacteria *(E. coli, S. typhimurium and P. aeruginosa*) and Gram-positive bacteria (*St. aureus*) and yeast *C. albicans* reached more than 75% indicating strong bactericidal agent toward Gram-negative and Gram-positive bacterial strains. Meanwhile, the CS-bioAgNP composite clearly shows the greatest inhibitory effect against all microbial growth strains in comparison with chitosan and other CS-bioNPs composites after 120 min of exposure. These results are consistent with the findings of Kaur et al. (2013). Similarly, Cao et al. (2010) reported the antibacterial activity of silver/chitosan nanocomposites against bacterial strains.

Table 2 Coded coefficient and Tukey's comparisons of metal effects on microorganisms inhibition zones

Term	Coef	SE coef	T-value	P value	Tukey's pairwise comparison
Microorganisms					
C. albicans	-0.920	0.962	-0.96	0.353	AB
E. coli	1.080	0.962	1.12	0.278	AB
P. aeruginosa	-0.920	0.962	-0.96	0.353	AB
Sal. typhimurium	-2.120	0.962	-2.20	0.043	B
St. aureus	-	-	-		A
Material					
CS	-4.320	0.962	-4.49	0.000	C
CS-FeNPs	-	-	-	-	C
CS-AgNPs	8.080	0.962	8.40	0.000	A
CS-CdNPs	-3.120	0.962	-3.24	0.005	C
CS-CuNPs	2.680	0.962	2.79	0.013	B

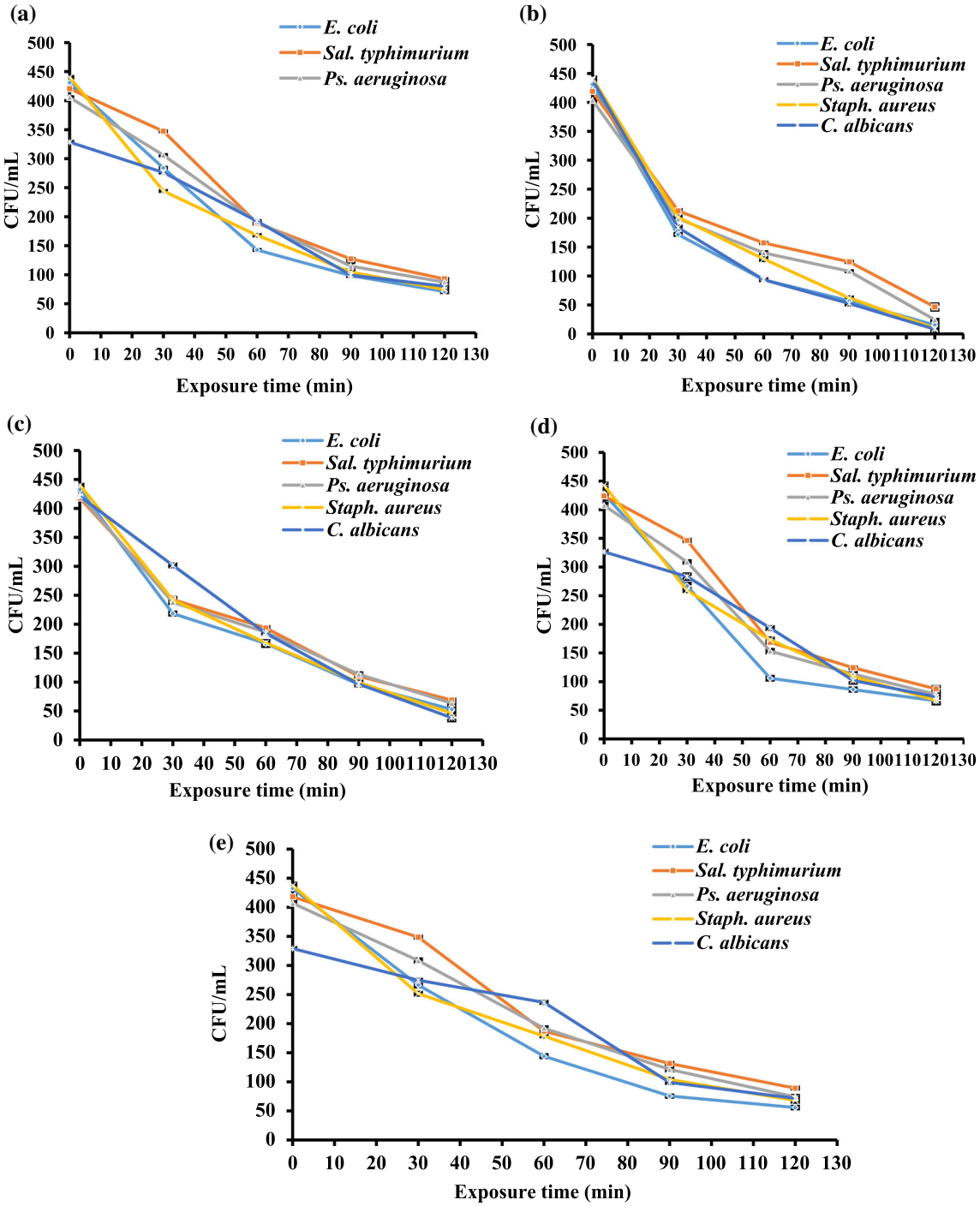

Fig. 9 Total bacterial counts (CFU/mL) of tested microbial strains survival after exposure to **a** chitosan (CS) **b** CS-Ag-nanocompostie **c** CS-Cu-nanocompostie **d** CS-Fe-nanocompostie **e** CS-Cd nanocompostie)

3.3.4 Statistical Analysis

The confidence intervals in Table 3 at 95%, both microorganisms and metal nanoparticles factors, were significant factors that affect the microorganism's reduction section where they recorded 0.002 and 0.000 < 0.05, respectively. Furthermore, Tukey's studies suggested that CS-Ag nanocomposite was the most significant metal that achieved high red microorganism reduction percent, followed by CS-Cu nanocomposite and the rest three metals in the last position. Table 4 shows the coded coefficient of the two-way ANOVA factor levels and the Tukey's comparison pairwise values.

Table 3 Percentage reduction of microbial growth caused after exposure to chitosan (CS) and different CS-bio-nanocomposites at 120 min

Microorganisms	Percentage reduction (%) of microbial growth (Mean ± SD)				
	CS	CS-Ag nanocomposite	CS-Cu nanocomposite	CS-Fe nanocomposite	CS-Cd nanocomposite
E. coli	83.72 ± 1.05	96.86 ± 1.75	88.14 ± 1.60	85.35 ± 1.32	87.33 ± 1.71
S. typhimurium	77.98 ± 1.30	89.76 ± 1.44	83.81 ± 1.54	79.88 ± 1.60	79.05 ± 1.48
P. aeruginosa	78.40 ± 1.23	93.95 ± 1.78	84.52 ± 1.23	81.36 ± 1.40	81.36 ± 1.48
St. aureus	83.18 ± 1.14	98.07 ± 1.30	89.20 ± 1.56	85.45 ± 1.70	85.00 ± 1.66
C. albicans	75.61 ± 1.11	98.64 ± 1.45	90.00 ± 1.72	78.05 ± 1.28	77.74 ± 1.22

SD is standard deviation

Table 4 Coded coefficient and Tukey's comparisons of metal effects on microorganisms reduction percent (%)

Term	Coef	SE coef	T-value	P value	Tukey's pairwise comparison
Microorganisms					
C. albicans	-1.288	0.937	-1.37	0.188	AB
E. coli	2.984	0.937	3.18	0.006	A
P. aeruginosa	-1.378	0.937	-1.47	0.161	AB
S. typhimurium	-3.200	0.937	-3.42	0.004	B
St. aureus	-	-	-	-	A
Material					
CS	-5.518	0.937	-5.89	0.000	C
CS-Ag nanocomposite	10.160	0.937	10.84	0.000	A
CS-Cd nanocomposite	-3.200	0.937	-3.42	0.004	C
CS-Cu nanocomposite	1.838	0.937	1.96	0.068	B
CS-Fe nanocomposite	-	-	-	-	C

4 Conclusions

In this study, the biosynthesis of different metal nanoparticles by four microbial strains *Salmonella typhimurium, Candida albicans, Fusarium avenaceum and Staphylococcus aureus* was determined. The smallest particle size was produced by *Salmonella typhimurium* when compared to other microbial synthesized nanoparticles. The silver nanoparticle was given the smallest size nanoparticle by *S. typhimurium* when compared with other metal nanoparticles. Hence, *S. typhimurium* was selected for further studies. The chemical modifications of chitosan are generally preferred to improve the polymer process. Hence, the biologically synthesized metal nanoparticles were immobilized on the chitosan (CS) giving CS-bio-nanocomposites for the enhancement of its antimicrobial and anticancer properties. Results showed that the CS-bio-nanocomposites significantly enhanced the cytotoxicity and antibacterial activities. The CS-bioAgNP composite clearly shows the greatest cytotoxicity activity against the tested three tumor cells and antimicrobial activities against all tested microbial strains in comparison with chitosan and other CS-bioNPs composites.

Authors' contributions H.S. El-Sheshtawy and M.F. Mady performed the biosynthesis of different nanoparticles by different microbial strains. The two authors also investigated the antimicrobial activity of the prepared CS-bio-nanocomposites against different microbial strains. **H.H.H. Hefni** performed the preparation of chitosan bio-nanocomposites. **Wael A. Aboutaleb** achieved the characterization of the prepared CS-bio-nanocomposites. **M.M. Elaasser** performed the cytotoxicity of the prepared CS-bio-nanocomposites against the tumor cells. All the authors contributed to the interpretation of the data in the manuscript and writing the manuscript. All authors read and approved the final manuscript. **H.H. El-Shiekh** performed the final revision of the manuscript.

Declarations

Conflict of interest The authors declare that they have no competing interests.

Consent to Participate All authors accepted for the participation of this manuscript.

Consent to Publish All authors accepted for publishing this manuscript.

References

Al-Ostoot FH, Vidya R, Mohammed YH, Jyothi M, Pallavi H, Khanum SA (2018) Statistical analysis of antimicrobial data of 2-[2-(Aroyl) aroyloxy] methyl-1, 3, 4 oxadiazoles analogues using ANOVA. Asian J Pharm 11:293–297

Asha-Rani PV, Mun GLK, Hande MP, Valiyaveettil S (2009) Cytotoxicity and genotoxicity of silver nanoparticles in human cells. ACS Nano 3:279–290

Avinash PI, Nelson D, Mahendra R (2014) Bioactivity, mechanism of action and cytotoxicity of copper-based nanoparticles: A review. Appl Microbiol Biotechnol 98:1001–1009

Badr EA, Shafek SH, Hefni HHH, Elsharif AM, Alanezi AA, Shaban SM, Kim DH (2021) Synthesis of Schiff base-based cationic Gemini surfactants and evaluation of their effect on in-situ AgNPs preparation: Structure, catalytic and biological activity study. J Molecr Liquids 326:115342

Balouiri M, Sadiki M, Ibnsouda SK (2016) Methods for in vitro evaluating antimicrobial activity: A review. J Pharm Anal. 4:71–79

Barry AL, Craig WA, Nadler H, Reller LB, Sanders CC, Swenson JM (1999) Methods for determining bactericidal activity of antimicrobial agents; approved guideline. NCCLS document M26-A. National Committee for Clinical Laboratory Standards, Wayne, PA

Bastos EM, Simone M, Jorge DM, Soares AE, Spivak MJ (2008) In vitro study of the antimicrobial activity of Brazilian propolis against Paenibacillus larvae. J Invert Pathol 97:273–281

Bong-Kyu C, Kwang-Yoon K, Yun-Jung Y, Suk-Jung O, Jong-Hoon C (2001) Chong-Youl Kim (2001) Int. J Antimicrob Agents 18:553–557

Cao XL, Cheng C, Ma YL, Zhao CS (2010) Preparation of silver nanoparticles with antimicrobial activities and the researches of their biocompatibilities. J Mat Sci: Mat Med 21:2861–2868

Chung YC, Su YP, Chen CC, Jia G, Wang HI, Wu JC, Lin JY (2004) Relationship between antibacterial activity of chitosan and surface characteristics of cell wall. Acta Pharm Sinica 25:932–936

Dakal TC, Kumar A, Majumdar RS, Yadav V (2016) Mechanistic basis of antimicrobial actions of silver nanoparticles. Front Microb. https://doi.org/10.3389/fmicb.2016.01831

Dutta PK, Rinki K, Dutta J (2011) Chitosan: a promising biomaterial for tissue engineering scaffolds. In: Chitosan for biomaterials II. Springer, pp 45–79

Ghorbani HR (2013) Biosynthesis of silver nanoparticles using *Salmonella typhirium*. J Nanostr Chem 3:29–32

Gu H, Ho PL, Tong E, Wang L, Xu B (2003) Presenting vancomycin on nanoparticles to enhance antimicrobial activities. Nano Lett 3:1261–1263

Hussein MHM, El-Hady MF, Sayed WM, Hefni H (2012) Preparation of some chitosan heavy metal complexes and study of its properties. Poly Sci Ser A 54(2):113–124

Jbeli A, Hamden Z, Bouattour S, Ferraria AM, ConceiÃÃ£o DS, Ferreira LF, Chehimi MM, do- Rego MB, Vilar MR, Boufi S, (2018) Chitosan-Ag-TiO_2 films: An effective photocatalyst under visible light. Carbohy Poly 199:31–40

Jin Y, Zhao X (2009) Cytotoxicity of photoactive nanoparticles. In: safety of nanoparticles. Springer, New York, pp 19–31. https://doi.org/10.1007/978-0-387-78608-7

Kathiresan K, Manivannan S, Nabeel MA, Dhivya B (2009) Studies on silver nanoparticles synthesized by a marine fungus, *Penicillium fellutanum* isolated from coastal mangrove sediment. Coll Surf b: Biointer 71:133–137

Kaur P, Choudhary A, Thakur R (2013) Synthesis of chitosan-silver nanocomposites and their antibacterial activity. Intern J Sci Engine Res 4(4):869–872

Kaur A, Preet S, Kumar V, Kumar R, Kumar R (2019) Synergetic effect of vancomycin loaded silver nanoparticles for enhanced antibacterial activity. Coll Surf B: Biointer 176:62–69

Khan I, Saeed K, Khan I (2019) Review Nanoparticles: properties, applications and toxicities. Arab J Chem 12:908–931

Kim KJ, Sung WS, Suh BK, Moon SK, Choi JS, Kim JG, Lee DG (2009) Antifungal activity and mode of action of silver nanoparticles on *Candida albicans*. Biom: J Role Met Ions Biol Biochem Med 22:235–242

Konaté K, Mavoungou JF, Lepengué AN, Aworet-Samseny RR, Hilou A, Souza A, Dicko MH, M'batchi B, (2012) Antibacterial activity against β-lactamase producing Methicillin and Ampicillin-resistants' *Staphylococcus aureus*: Fractional Inhibitory Concentration Index (FICI) determination. Ann Clini Microbiol Antimicro 11:1–29

Kong L, Gao Y, Cao W, Gong Y, Zhao N, Zhang X (2005) Preparation and characterization of nanohydroxyapatite/chitosan composite scaffolds. J Biom Mat Res Part a: Offi J Soci Bioma Jap Soc Bioma Aust Soc Bioma Kor Soc Bioma 75:275–282

Kumar R, Sharma P, Bamal A, Sushma Negi S, Chaudhary S (2017) A safe, efficient and environment friendly biosynthesis of silver nanoparticles using Leucaena leucocephala seed extract and its antioxidant, antimicrobial, antifungal activities and potential in sensing. Green Process Synth 6:449–459

L'Azou B, Passagne I, Mounicou S, Tréguer-Delapierre M, Puljalté I, Szpunar J, Ohayon-Courtès C (2014) Comparative cytotoxicity of cadmium forms ($CdCl_2$, CdO, CdS micro-and nanoparticles) in renal cells. Toxicol Res 3(1):32–41

Li J, Tang X, Yi H, Yu Q, Gao F, Zhang R, Li C, Chu C (2017) Effects of copper-precursors on the catalytic activity of Cu/graphene catalysts for the selective catalytic oxidation of ammonia. Appl Surf Sci 412:37–44

Li-Feng Q, Zi-Rong X, Yan L, Xia J, Xin-Yan H (2005) In-vitro effects of chitosan nanoparticles on proliferation of human gastric carcinoma cell line MGC803 cells. World J Gastroentero 11(33):5136–5514

Liu Y, Babu HV, Zhao J, GoÃi-Urtiaga A, Sainz R, Ferritto R, Pita M, Wang DY (2016) Effect of Cu-doped graphene on the flammability and thermal properties of epoxy composites. Comp Part b: Engin 89:108–116

Mandal D, Bolander ME, Mukhopadhyay D, Sarkar G (2006) The use of microorganism for the formation of metal nanoparticles and their application. Appl Microbiol Biotechnol 69(5):485–492

Mlalila NG, Swai HS, Hilonga A, Kadam DM (2017) Antimicrobial dependence of silver nanoparticles on surface plasmon resonance bands against Escherichia coli. Nanotechnol Sci Applic 10:1–9

Mohsena E, El-Borady OM, Mohamed MB, Fahim IS (2020) Synthesis and characterization of ciprofloxacin loaded silver nanoparticles and investigation of their antibacterial effect. J Radi Res Appl Sci 13(1):416–425. https://doi.org/10.1080/16878507.2020.1748941

Motawie AM, Mahmoud KF, El-Sawy AA, Kamal HM, Hefni H, Ibrahiem HA (2014) Preparation of chitosan from the shrimp shells and its application for pre-concentration of uranium after cross-linking with epichlorohydrin. Egy J Petro 23:221–228

Mott D, Galkowski J, Wang L, Luo J, Zhong CJ (2007) Synthesis of size-controlled and shaped copper nanoparticles. Langmuir 23:5740–5745

Mukherjee PS, Das AK, Dutta B, Meikap AK (2017) Role of silver nanotube on conductivity, dielectric permittivity and current

voltage characteristics of polyvinyl alcohol-silver nanocomposite film. J Phys Chem Sol 111:266–273
Muzzarelli RA, Tarsi R, Filippini O, Giovanetti E, Biagini G, Varaldo P (1990) Antimicro Agents Chemother 34:2019–2033
Ovais M, Khalil AT, Ayaz M, Ahmad I, Nethi SK, Mukherjee S (2018) Review: Biosynthesis of metal nanoparticles via microbial enzymes: A mechanistic approach. Intern J Mole Sci 19(12):4100–4120
Pérez-Herrero E, Fernández-Medarde A (2015) Advanced targeted therapies in cancer: drug nanocarriers, the future of chemotherapy. Euro J Pharm Biopharm 93:52–79
Pujalté I, Passagne I, Brouillaud B, Tréguer M, Durand E, Ohayon-Courtès C, L'Azou B (2011) Cytotoxicity and oxidative stress induced by different metallic nanoparticles on human kidney cells. Part Fiber Toxicol 8(1):10–17
Raffi M, Hussain F, Bhatti TM, Akhter JI, Hameed A, Hasan MM (2008) Antibacterial characterization of silver nanoparticles against *E. coli* ATCC-15224. J Mat Sci Technol 24:192–196
Roller S, Covill N (1999) The antifungal properties of chitosan in laboratory media and apple juice. Int J Food Microbiol 73:672–681
Satyavani K, Gurudeeban S, Ramanathan T, Balasubramanian T (2011) Biomedical potential of silver nanoparticles synthesized from calli cells of Citrullus colocynthis (L) Schrad. J Nanobiotechnol. 9(43):2–8
Schrand AM, Rahman MF, Hussain SM, Schlager JJ, Smith DA, Syed AF (2010) Metal-based nanoparticles and their toxicity assessment. Wires Nanomed Nanobiotechnol 2(5):544–568
Shahverdi AR, Fakhimi A, Shahverdi HR, Minaian S (2007) Synthesis and effect of silver nanoparticles on the antibacterial activity of different antibiotics against *Staphylococcus aureus* and *Escherichia coli*. Nanomed Nanotechnol Biol Med 3(2):168–171
Sriram MI, Kanth SB, Kalishwaralal K, Gurunathan S (2010) Antitumor activity of silver nanoparticles in Dalton's lymphoma ascites tumor model. Intern J Nanomed 5:753–762
SuÃrez-Cerda J, Espinoza-GÃmez H, Alonso-NÃÃez G, Rivero IA, Gochi-Ponce Y, Flores-LÃpez LA (2017) A green synthesis of copper nanoparticles using native cyclodextrins as stabilizing agents. J Saudi Chem Soc 21:341–348
Sunkar S, Nachiyar CV (2012) Biogenesis of antibacterial silver nanoparticles using the endophytic bacterium *Bacillus cereus* isolated from *Garcinia xanthochymus*. Asi Paci J Trop Biomedi 2(12):953–959
Thomas V, Yallapu MM, Sreedhar B, Bajpai SK (2009) Fabrication, characterization of chitosan/nanosilver film and its potential antibacterial application. J Biomt Sci Poly Edit 20:2129–2144
Torres SK, Campos VL, LeÃ CG, RodrÃ-guez-Llamazares SM, Rojas SM, Gonzalez M, Smith C, Mondaca MA, (2012) Biosynthesis of selenium nanoparticles by *Pantoea agglomerans* and their antioxidant activity. J Nanopar Res 14(11):1236–1245. https://doi.org/10.1007/s11051-012-1236-3
Usman MS, Ibrahim NA, Shameli K, Zainuddin N, Yunus WM (2012) Copper nanoparticles mediated by chitosan: synthesis and characterization via chemical methods. Mole 7(12): 14928–14936
Vasileva P, Donkova B, Karadjova I, Dushkin C (2011) Synthesis of starch-stabilized silver nanoparticles and their application as a surface plasmon resonance-based sensor of hydrogen peroxide. Coll Surf a: Physic Engin Asp 382:203–210
Wang X, Du Y, Li H (2004) Preparation, characterization and antimicrobial activity of chitosan Zn complex. Carbohy Poly 56:21–26
Wei D, Sun W, Qian W, Ye Y, Ma X (2009) The Synthesis of Chitosan-Based Silver Nanoparticles and Their Antibacterial Activity Carbohydrate Research 344:2375–2382
Xia T, Kovochich M, Brant J, Hotze M, Sempf J, Oberley T, Sioutas C, Yeh J, Wiesner M, Nel A (2006) Comparison of the abilities of ambient and manufactured nanoparticles to induce cellular toxicity according to an oxidative stress paradigm. Nano Lett 6:1794–1807
Yasmin S, Nouren S, Bhatti HN, Iqbal DN, Iftikhar S, Majeed J, Mustafa R, Nisar N, Nisar J, Arif Nazir A, Iqbal M, Rizvi H (2020) Green synthesis, characterization and photocatalytic applications of silver nanoparticles using *Diospyros lotus*. Gre Proces Synth 9:87–96
Yuvakkumar R, Elango V, Rajendran V, Kannan N (2011) Preparation and characterization of zero valent iron nanoparticles. Dig J Nanomat Biostruc 6:1771–1776